

Regeneration and anti-migration of sand waves associated with sand mining in the Taiwan Shoal

Jingjing Bao^{1,2}, Feng Cai^{1,3*}, Chengqiang Wu^{1,2}, Huiquan Lu^{1,2}, Yongling Zheng^{1,2}, Yufeng Li⁵, Li Sun^{1,4}, Chungeng Liu^{1,4}, Yongbao Li^{1,4}

¹Laboratory of Ocean and Coast Geology, Third Institute of Oceanography, Ministry of Natural Resources, Xiamen 361005, China

²Fujian Provincial Key Laboratory of Marine Physical and Geological Processes, Xiamen 361005, China

³Fujian Provincial Key Laboratory of Marine Ecological Protection and Restoration, Xiamen 361005, China

⁴Xiamen Ocean Engineering Exploration and Design Institute Co. Ltd., Xiamen 361005, China

⁵School of Environment and Resource, Southwest University of Science and Technology, Mianyang 621010, China

Received 7 October 2022; accepted 6 December 2022

© Chinese Society for Oceanography and Springer-Verlag GmbH Germany, part of Springer Nature 2023

Abstract

Sand waves in the Taiwan Shoal are characterized by two distinct spatial scales. Giant sand waves have a length of 2 kilometers with height between 5 m and 25 m, whilst small sand waves is less than 100-m long with height less than 5 m between giant sand wave peaks (crests). A series of five high-resolution multi-beam echo-sounding surveys between 2012 and 2020 in the middle of Taiwan Shoal indicated that artificial dredging on the giant sand waves had caused sand wave reform and evolution. Overall, the removal of giant sand waves significantly affected the migration of small sand waves adjacent to the dredging site, with the latter on both sides of the former appear to migrate towards the dredging pit. Moreover, in the dredging area, new sand waves emerged with wavelength much smaller than the original giant sand waves, while the convergent pattern of the small sand waves tends to store and form the giant sand waves, which might spread far beyond the survey period.

Key words: small sand wave, giant sand wave, anti-migration, regrowing, sand mining, Taiwan Shoal

Citation: Bao Jingjing, Cai Feng, Wu Chengqiang, Lu Huiquan, Zheng Yongling, Li Yufeng, Sun Li, Liu Chungeng, Li Yongbao. 2023. Regeneration and anti-migration of sand waves associated with sand mining in the Taiwan Shoal. *Acta Oceanologica Sinica*, 42(9): 71–78, doi: 10.1007/s13131-023-2162-1

1 Introduction

Large sand waves delimited for active bedload movement by coastal professions, are a fascinate feature in the ocean. They are rhythmic bed form that have been observed globally in many tide-dominated shallow continental shelves (Van de Meene et al., 1996; Off, 1963; Terwindt, 1971; McCave, 1971; Liu et al., 1998; Bao et al., 2014). Spatiotemporal variation in hydrodynamic conditions has been recognized as a dominant factor which accounts for the differences in the formation and evolution of sand waves (Off, 1963; Hulscher, 1996; Berné et al., 2002; Campmans et al., 2017, 2018; Bao et al., 2020), while increasing socio-economic development has aggravated the impact of anthropogenic activities on the dimensions and evolution of sand waves (Verboven, 2017). Besides the increasing scientific interest in the characteristics and evolution of sand waves, the understanding gained from research in this subject is valuable for dredging operations, such as for maintenance of navigation channels and marine sand mining (Hulscher et al., 2000; Knaapen et al., 2000, 2002).

Many previous studies on sand waves have focused on analyzing and estimating the evolution of sand waves using numerical models. For example, Hulscher et al. (2000) applied a simple model to estimate the recovery of sand wave amplitude and to

evaluate different dredging strategies. Knaapen et al. (2000, 2002) combined the Landau model and a genetic algorithm to predict the regeneration of sand waves in a field dredging experiment in the Bisanseto Sea, Japan. Verboven (2017) also used a numerical model to predict the regeneration process of a tide-induced sand wave after dredging on the Kwinte Bank in Belgian North Sea and discussed practical applications in different places. In addition, Campmans et al. (2021) presented a process-based model study to examine the recovery of sand waves under different dredging strategies (topping and swiping), which affect their height and shape. However, most of the previous studies tended to ignore the process response of the seabed topography at a dredging site and its adjacent area.

In this paper, the recovery of the sand wave is analyzed employing the dataset of five biennial field observations during 2012–2020 at Taiwan Shoal in the south of Taiwan Strait, a 180 km wide channel. The strait that connects the East China Sea to the South China Sea is abundant in sand waves, especially at Taiwan Shoal, has been affected by a complex hydrodynamic system composing tidal currents, a branch of the Kuroshio Current, the northward South China Sea Warm Current and southward China Coastal Current (Wang et al., 2003; Hong et al., 2009; Hu et al.,

Foundation item: The Scientific Research Foundation of Third Institute of Oceanography, Ministry of Natural Resources under contract Nos 2018028, 2019005 and 2019018; the Science and Technology Project in Fujian Province, China under contract No. 2021H0041.

*Corresponding author, E-mail: fcai800@126.com

2010). The tides on the Taiwan Shoal are primarily irregular semidiurnal, and the M_2 tide with a range of 0.8–1.0 m/s is a predominant constituent propagating from the Pacific Ocean into the Taiwan Strait (Liu et al., 1998; Du et al., 2010). The East Asia monsoon (southeasterly in summer and northeasterly in winter) has significant effect on local wave climate (Bao et al., 2020), especially in winter, when the northeast winds tend to drive strong flow southwards (Wang et al., 2021), causing an intermittent counter-wind current in this area (Chuang et al., 1993; Oey et al., 2014; Chen et al., 2016; Li et al., 2018; Shen et al., 2017, 2019; Hu et al., 2019).

Marine sand has been mined for various purposes, as building materials or for road construction. Consequently, concern on its environmental impacts has arisen to investigate the regeneration of sand waves on the Taiwan Shoal after sand mining in the central south of the Taiwan Strait, where rhythmic giant sand waves (GSWs) and small sand waves (SSWs) have co-existed (Fig. 1). A large-scale sand dredging operation in 2016 caused severe disruption to the rhythmic sea bed, fragmenting some sand waves. Five biennial surveys over a period of eight years (2012–2020) have shown the shape of the GSWs had remained relatively stable before dredging, but evolved into several SSWs soon after each dredging.

The present paper is structured as follows. After a brief introduction in Section 1, Section 2 presents the observation data and Section 3 describes the changes to the GSWs and migration of the SSWs. Section 4 discusses the evolution of the GSWs and the SSWs after dredging, as well as examines the hypotheses for sand wave migration and shape asymmetry. Finally, conclusions are given in Section 5.

2 Field observations

Taiwan Shoal is in the south of Taiwan Strait, which has an

area about 13 000 km² and located within 20–50 m beneath the mean sea level. The present study collates the results of five sand wave monitoring surveys in 2012 to 2020 within an area of 2.5 km × 8 km in the central Taiwan Shoal (Fig. 1). Bathymetric data (multi-beam) were collected biennially by R2Sonic 2024 (256 beams/ping, 400 kHz) and ResonSeabat 7125 (512 beams/ping, 400 kHz) during 2012–2016 and 2018–2020, respectively. Navigation during data collection was facilitated by Veripos GPS for the horizontal grids and tide gauges with accuracy within ±10 cm and ±20 cm, respectively. The raw multi-beam bathymetric data were then processed by CARIS HIPS and SIPS software (CARIS, Inc., 2012; Caris HIPS and SIPS, V7.1.2) with correction in sound velocity and tide, for quality control. The accuracy of the final bathymetric data satisfies the standard of S-44 (the special order of the International Hydrographic Organization) (IHO, 2008).

The present study focuses on a feature region of 1 400 m × 1 800 m (the small rectangular box within Taiwan Shoal; Fig. 1) for the biennial survey to enhance the analysis of dredging and regeneration of the sand waves. A Digital Terrain Model (DTM) was constructed using the Fledermaus software (Interactive Visualization Systems Inc. 2009; Fledermaus, V7) for all five surveys conducted in June 2012, July 2014, July 2016, August 2018, and July 2020 (shown in Figs 2a–e, respectively). The crest lines denoting the location and alignment of the GSWs (KL) and SSWs (MN) are indicated in the feature region, while the profiles of the crest lines KL and MN are presented separately in Fig. 3 for clarity.

3 Results

The results of the high-resolution DTM and nuanced crest lines shown in Figs 2 and 3 reveal the location and profiles of both GSWs and SSWs in the central Taiwan Shoal and the mor-

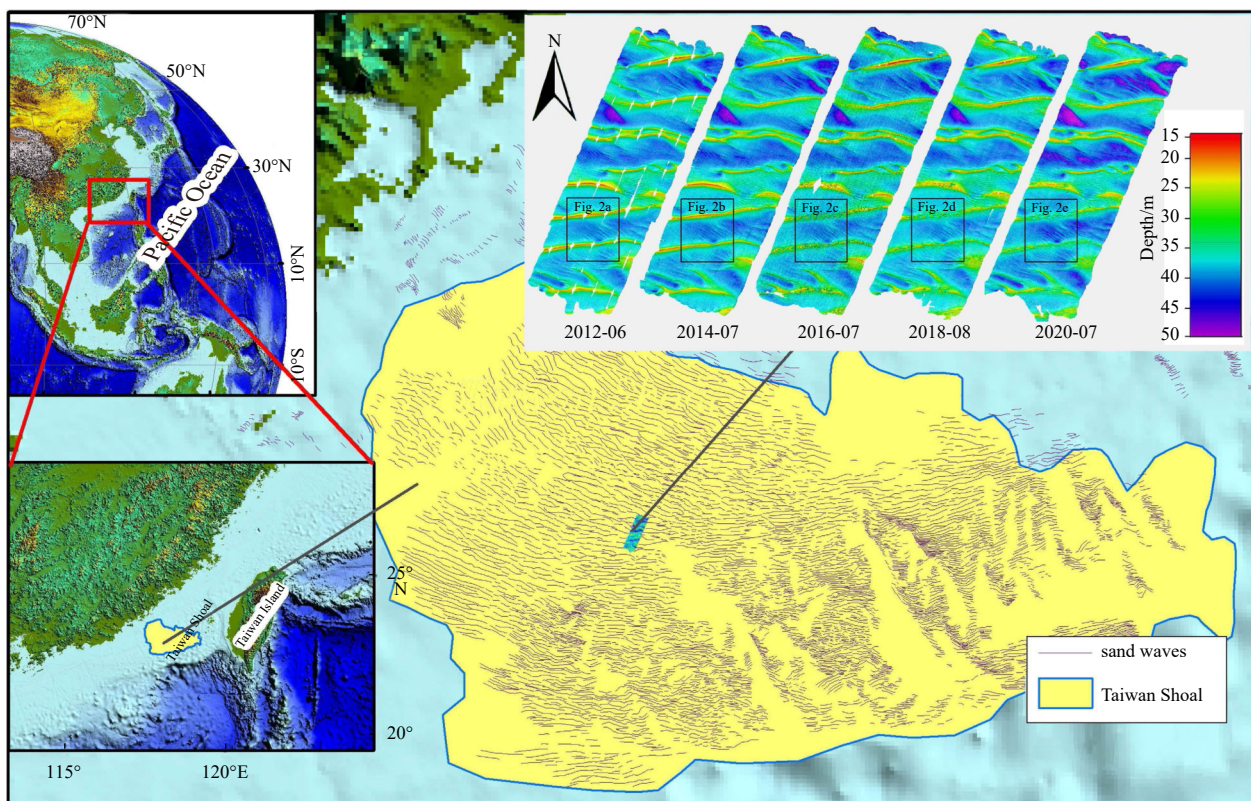


Fig. 1. Location of Taiwan Shoal in the south of Taiwan Strait, showing sand wave dredging site (modified from Bao et al. (2020)).

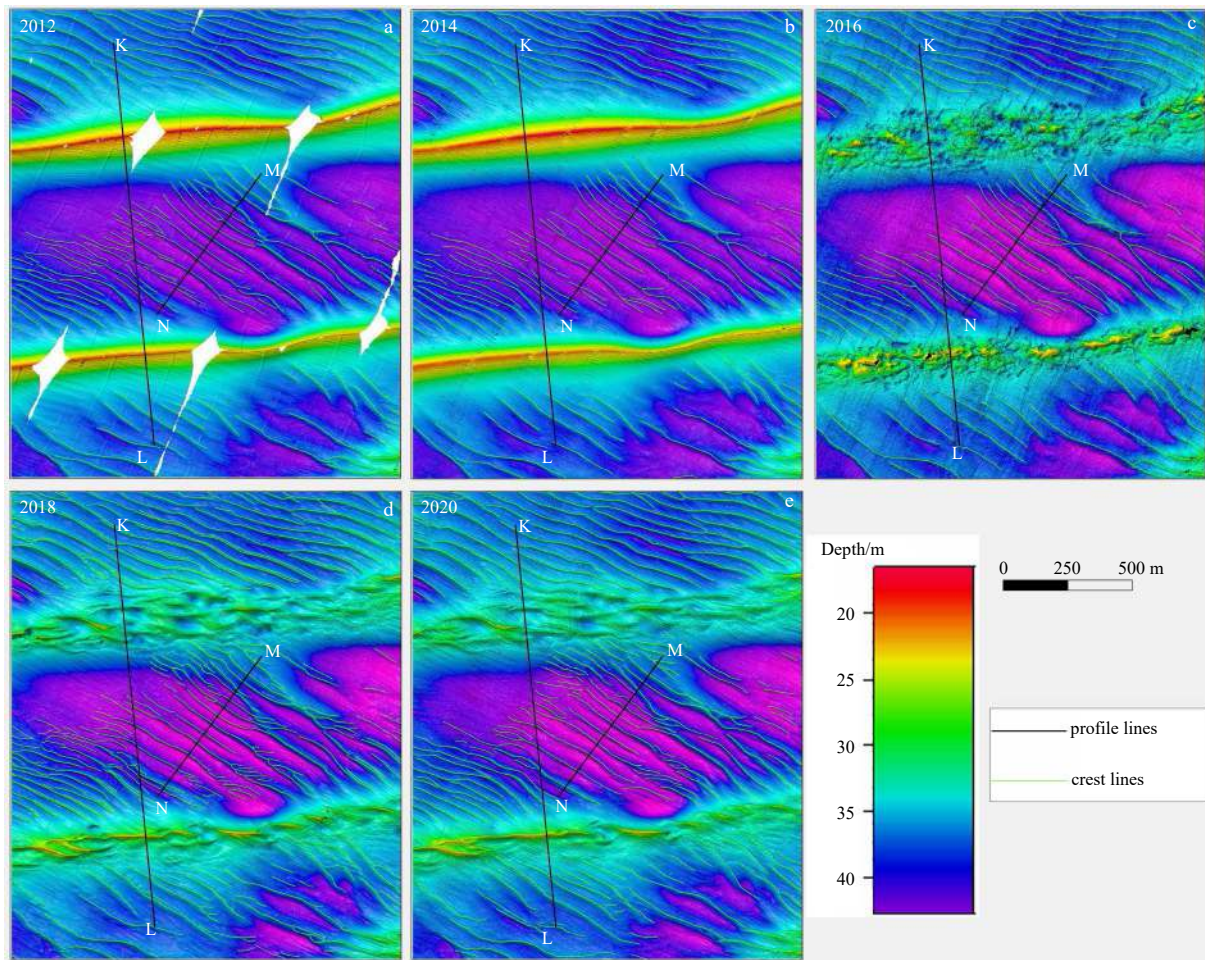


Fig. 2. Results of a digital terrain model for the five surveys during 2012–2020, showing crest line alignments of the giant sand waves (KL) and small sand waves (MN) plus multiple profiles in the feature region.

phology changes to the GSWs before and after a sand dredging operation.

3.1 Changes to giant sand waves

Figures 2a and b display the results of the DTM with the crest lines of the GSWs before each sand dredging during the summer in June 2012 and July 2014, respectively, in which “SW-A” and “SW-B” (in the north and south of the feature region) appeared to remain relatively stable over the observation period. However, slight changes occurred, showing the migration of the GSWs northward in perpendicular to their crestlines at the rate of 1–5 m/a during 2012 to 2014 (which was calculated by measuring data at different year). On the contrary, after the large-scale sand dredging during 2015–2016, the body of SW-A was almost completely excavated and its shape was destroyed as well (Fig. 2c). Reduction in crest height over 15 m was detected and average landform height decreased by 2.31 m, whereas dredging at SW-B reduced its crest height over 7 m and average height by 0.87 m. However, despite the reduction in height, the sand wave shape of the SW-B remained almost identical (Fig. 3a).

The morphology of both dredging areas (i.e., SW-A and SW-B) evolved between 2016 and 2018. During the first two years after dredging, the resulting uneven landform gradually disintegrated into many SSWs lying parallel to the original GSWs (Fig. 4), reaching a total of 33 or more in 2018. In Fig. 4, the depth vari-

ation represents the sounding results between two adjacent measurements. Over the next two years (2018–2020), these SSWs experienced local evolution, from gradual merging of multiple SSWs to migration northward in perpendicular to their crestlines at the speed of 1–5 m/a. However, their general shape was retained.

3.2 Migration of small sand waves

The SSWs within the troughs of GSWs in the feature area had different motion characteristics before and after dredging. The migration could be divided into two stages by comparing the multiple crest lines (Fig. 5) and the multiple crest profiles (Line MN in Figs 2 and 3b) in the feature region (Fig. 3a).

Stage 1 (before dredging in 2016): Comparison between the DTM result and crest lines between 2012 and 2014 indicates SSWs remained relatively stable with a consistent shape, despite slight variations in elevation and locations, while migrating northeastward. Meanwhile, some SSWs near the northern slope of the GSWs tended to migrate southwestward (Figs 5b,3b).

Stage 2 (after dredging in 2016): As shown in Fig. 5a, most of the crest lines of the SSWs migrated southwestward, in perpendicular to their crestlines at the speed of 2–10 m/a. Eventually, the number of SSWs increased, expanding into the area of SW-A during 2016–2020. However, the rate of migration gradually decreased from southwest (up to 10 m/a) toward the central area (about 1–3 m/a), and even reversed northeasterly close to another

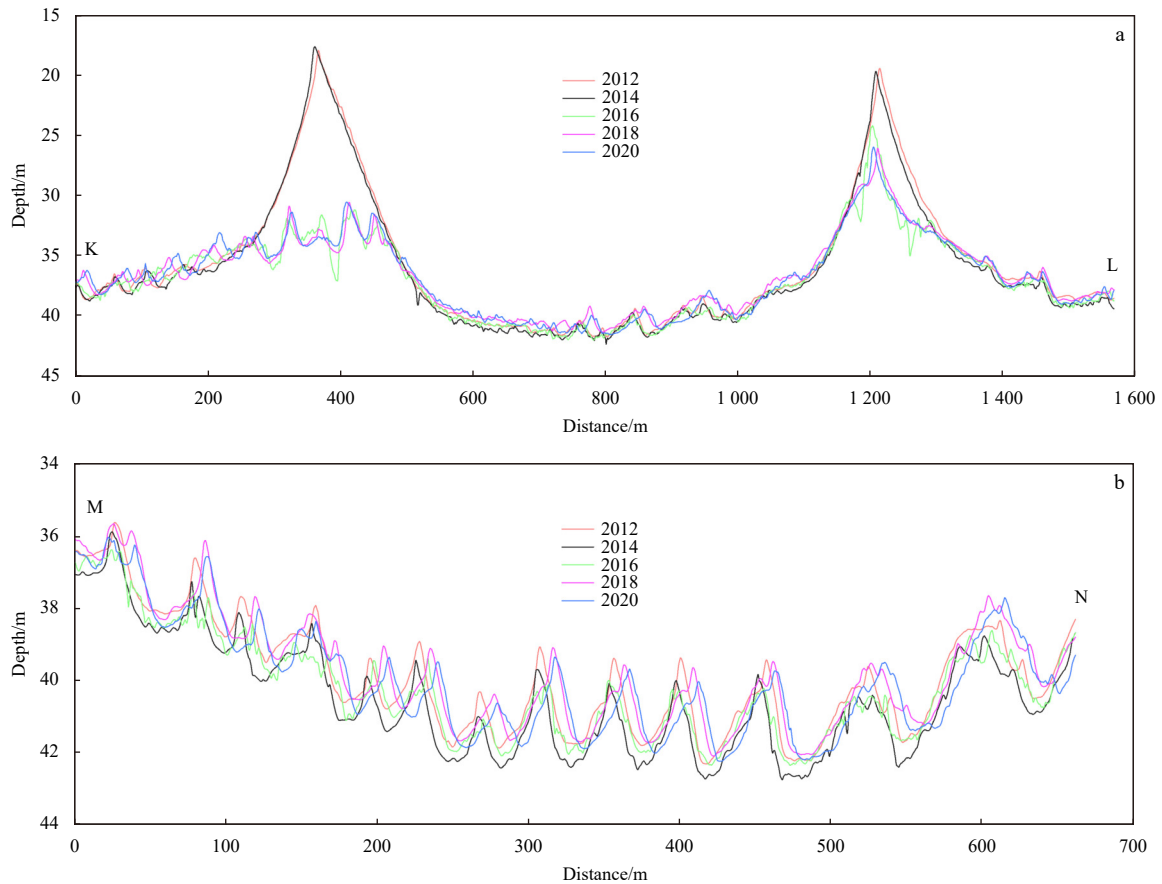


Fig. 3. Crest line profiles of KL for the giant sand waves (a) and MN for the small sand waves (b) in the five surveys during 2012 and 2020 (refer to Fig. 2)

er GSW (Figs 5c–e). As shown in Fig. 3b, the SSWs migrated southwestward in perpendicular to their crest lines from their perspective multiple profiles.

4 Discussions and hypotheses

4.1 Evolution of giant sand waves

Figure 4 displays the spatiotemporal variations of the mean height difference in the dredged area SW-A, where the GSWs were affected by seasonal local currents, as well as many other environmental factors (e.g., tropical storms, internal waves and artificial dredging). For example, Bao et al. (2020) applied a Morlet wavelet function and found storm could change the shape of the SSWs and reduce the crests of the GSWs, though bedforms might recover afterward. This infers that the mean height difference of -0.39 m (Fig. 4) in the sand waves could be attributed to the erosion by storms and the incomplete recovery of sand waves between 2012 and 2014. In addition, dredging also reduced the mean height by 2.31 m during 2015–2016, which had significantly changed the depth and shape of the GSWs. On the other hand, the observed mean height increase of 0.30 m (Fig. 4) represents partial recovery of the dredging pit in the GSWs under the action of tidal currents after the first two years of dredging (2016–2018). Furthermore, the insignificant mean height difference of -0.06 m over the subsequent two years (2018–2020; Fig. 4) indicated gradual stabilization in the giant sand wave area. After all, artificial dredging could be the culprit for causing destruction of sand waves in the Taiwan Shoal.

4.2 Migration of small sand wave post dredging

Comparison on the multiple SSW crest lines in the troughs of GSWs reveals that SSWs have remained relatively stable, with a tendency of northeasterly migration before dredging. Zhou et al. (2018) divided the Taiwan Shoal into north and south subareas, separated by the giant sand wave Orientation Changing Limit (OCL), and concluded that North of the OCL comprises mainly NW–SE trending giant sand waves, and to the south of the OCL the giant sand waves are mainly W–E trending. Since the study area of the present study is in the north of the OCL, the results obtained from the present observations before dredging are in good agreement with that of Zhou et al. (2018). However, the direction of migration in the SSWs after dredging was found opposite to that before dredging (except where very close to the GSWs). Many previous observations elsewhere in the direction of sand wave migration also suggested a similar reversal under certain conditions. For example, Harris (1991) reported an asymmetrical shape of sand waves after the reversal of migration direction due to seasonal changes in the direction of the wind-driven current. Besio et al. (2004) proposed that tidal constituents could result in sand wave migration in a direction opposite to that of the net (residual) tidal current. Moreover, Hanes (2012) investigated the reversal of sand wave shape and migration direction in the San Francisco Bay. However, the results of these studies explicitly imply that the direction of sand wave migration after reversal often corresponded to the change in shape. To the contrary, the results in the present study indicate that sand waves could still retain their original shape in the course of reversal in direction (Fig. 6).

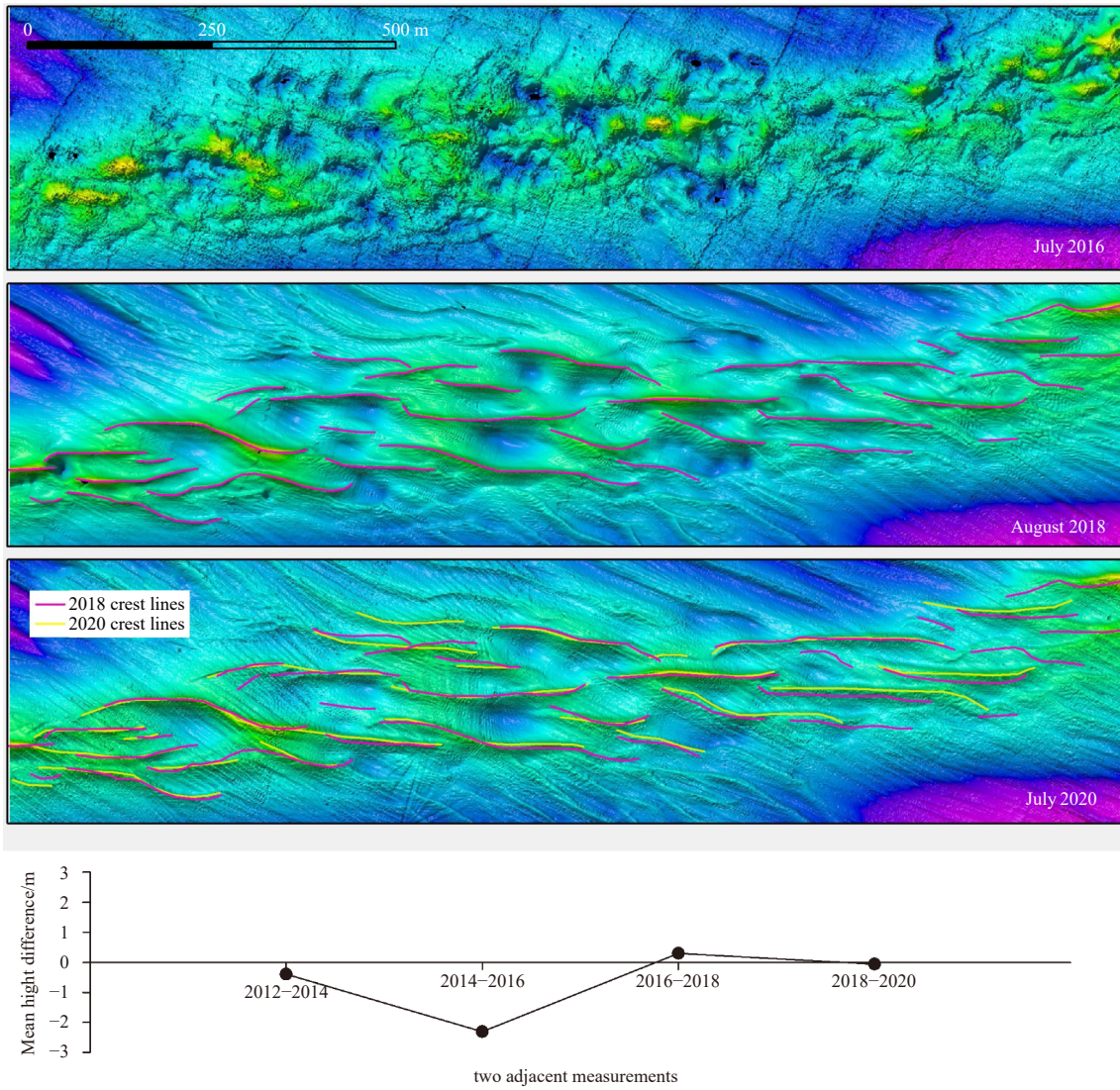


Fig. 4. Evolution of dredged area SW-A and the variation in mean height difference between two consecutive measurements (“+” for sedimentation, “-” for erosion).

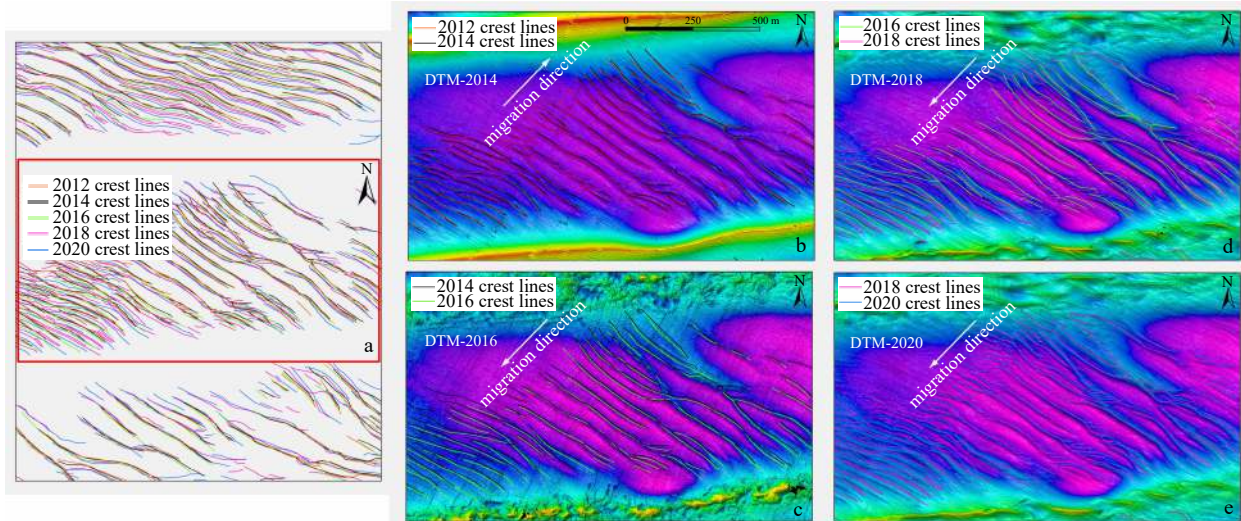


Fig. 5. Movement of multiple small sand wave crest lines in the troughs of giant sand waves in the feature region. DTM: Digital Terrain Model.

4.3 Hypotheses for migration and opposite to shape asymmetry

As mentioned above, artificial dredging had caused a reversal in migration of the SSWs, while their asymmetric shapes remained unchanged. This is a novel outcome arisen from the present study which must be validated by rational hypotheses.

The reversal in migration direction of the SSWs in the troughs of GSWs can be attributed to the converging migration of sand waves (Fig. 7) within the process of recovery of the GSWs. Fortunately, the results of previous studies have established a consensus that sand wave dredging can be used to restore an unstable seabed (Katoh et al., 1998; Knaapen and Hulscher, 2002; Verboven, 2017; Campmans et al., 2021). The present study adopts the crest line of a GSW in 2012 as a specific reference and divides the entire line into 20 divisions of 20 m each evenly distributed on the south and north slopes of the GSWs (Fig. 7). The height variation of each division is calculated by comparing their depths in 2016, 2018 and 2020, respectively. The resulting red and blue stakes in the histogram on the right-hand side of Fig. 7 show the erosion and siltation zones occurring on the north side of NB-10 and south side of SB-10 in the original GSW. The mean

high difference in these region (NB-07 and SB-08) was located on the north side of the crest line of the GSW, which corresponded to the gathering position of the crest lines of the SSWs. This supports the finding that GSWs were undergoing recovery after dredging.

The SSWs in the troughs of GSWs migrated in the direction opposite to that indicated by their shape asymmetry. This proposal is supported by the results as following:

(1) Several previous studies focused on a north–south rectilinear tidal current and a north directed long-term mean current in the Taiwan Strait during summer (Liu et al., 1998; Du et al., 2010; Bao et al., 2014).

(2) The China Coastal Current, the northward South China Sea Warm Current, together with a branch of the Kuroshio Current regulate the seasonal variations in the oceanic circulation in the Taiwan Strait (Jan and Chao, 2003; Wang et al., 2003; Hong et al., 2009; Zhou et al., 2018; Bao et al., 2020).

(3) A hydrodynamic change in the tidal current direction probably occurs due to northerly winds in winter or storms in summer. The dominant northeast winds tend to drive the flow south-

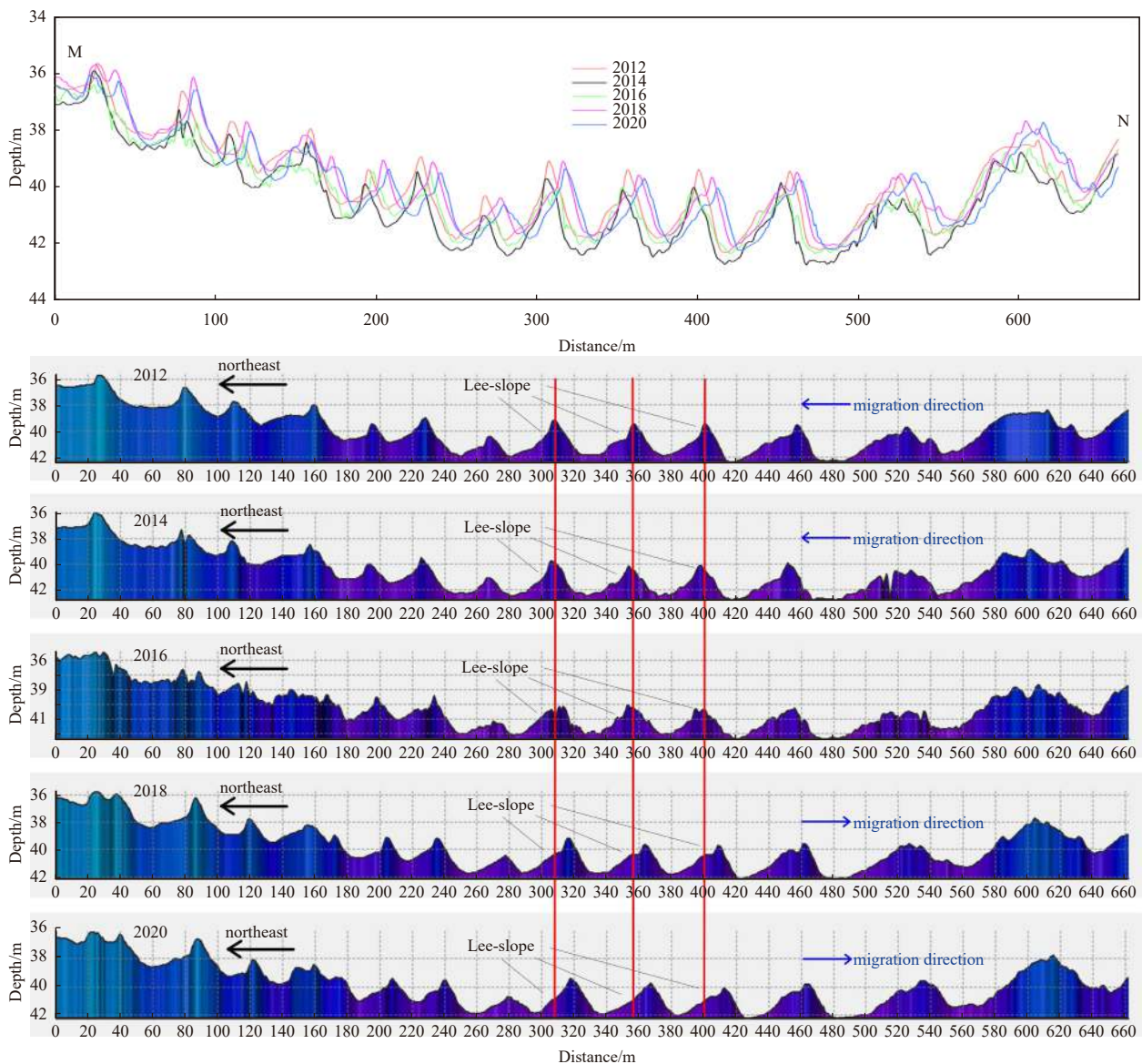


Fig. 6. Profiles of sand waves across the small sand waves in the troughs of giant sand waves.

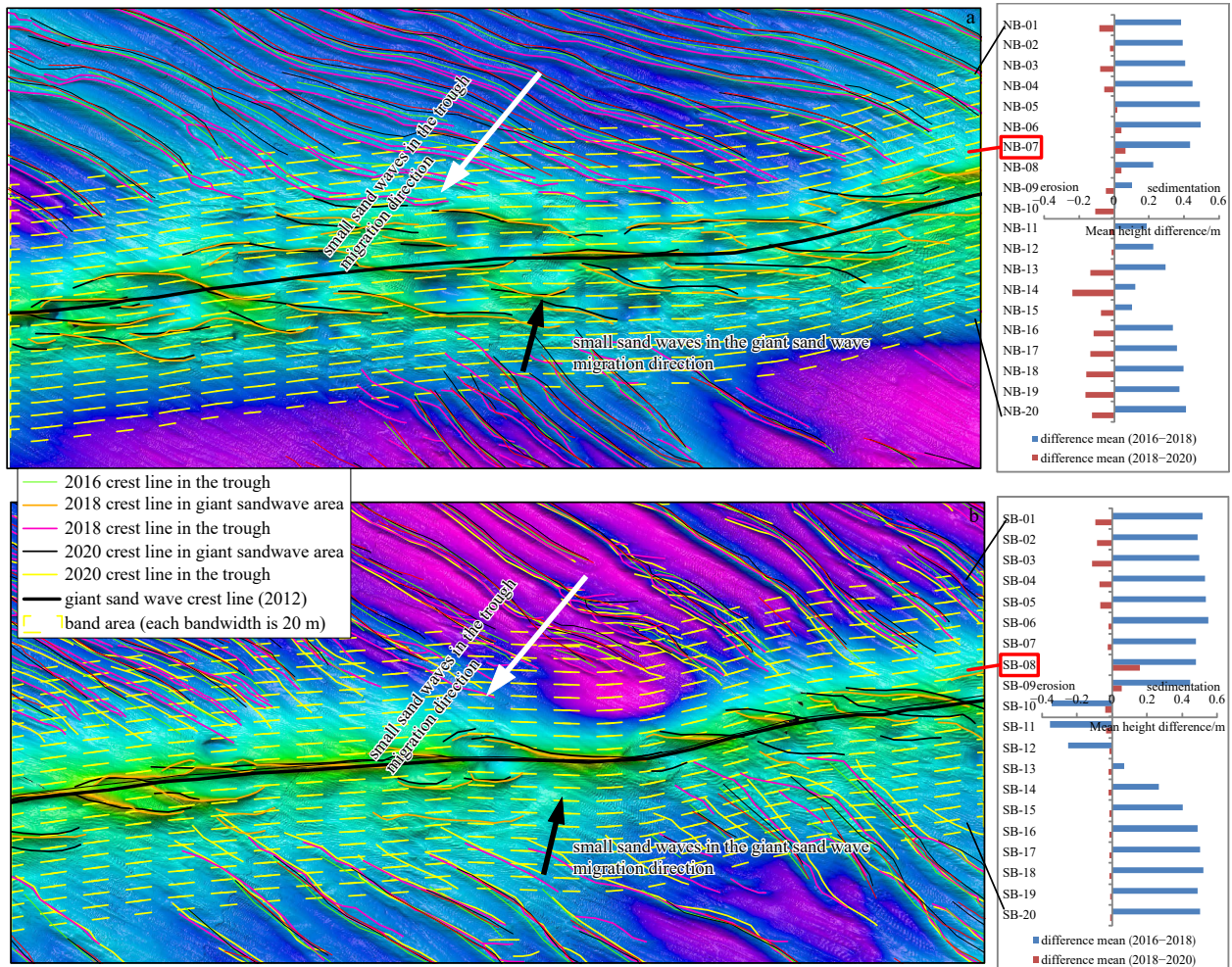


Fig. 7. Converging migration of both giant sand waves and small sand waves after dredging, showing distribution of 20 divisions (yellow strip area) consisting of sedimentation and erosion.

wards in winter (Wang et al., 2021). Meanwhile, depending on the strength of the wind, the intermittent appearance of a counter-wind current is another prominent feature (Chuang et al., 1993; Oey et al., 2014; Chen et al., 2016; Shen et al., 2017, 2019; Hu et al., 2019).

(4) Artificial dredging changed sea bottom topography either in height or in landform, which reflects the change in hydrodynamics (e.g., direction of the current in the troughs of GSWs), as well as in the shape and migration of sand waves.

5 Conclusions

A series of high-resolution multi-beam echo-sounding surveys within the Taiwan Shoal from 2012 to 2020 revealed that: dredging was the culprit in causing destruction to the GSWs in the study area, on which partial recovery was later provided by SSWs.

After dredging, uneven landforms gradually evolved into SSWs parallel to the original GSWs, while reversal in migration of the SSWs retained their original asymmetrical shape.

Converging migration was detected among the SSWs (between GSWs) and the dismantled GSWs during the recovery process, which may spread beyond the survey period.

Acknowledgements

We thank John Hsu, Fengyan Shi and Shaohua Zhao for detailed and constructive comments.

References

- Bao Jingjing, Cai Feng, Ren Jianye, et al. 2014. Morphological characteristics of sand waves in the middle Taiwan Shoal based on multi-beam data analysis. *Acta Geologica Sinica* (English Edition), 88(5): 1499–1512, doi: [10.1111/1755-6724.12314](https://doi.org/10.1111/1755-6724.12314)
- Bao Jingjing, Cai Feng, Shi Fengyan, et al. 2020. Morphodynamic response of sand waves in the Taiwan Shoal to a passing tropical storm. *Marine Geology*, 426: 106196, doi: [10.1016/j.margeo.2020.106196](https://doi.org/10.1016/j.margeo.2020.106196)
- Berné S, Vagner P, Guichard F, et al. 2002. Pleistocene forced regressions and tidal sand ridges in the East China Sea. *Marine Geology*, 188(3–4): 293–315, doi: [10.1016/S0025-3227\(02\)00446-2](https://doi.org/10.1016/S0025-3227(02)00446-2)
- Besio G, Blondeaux P, Brocchini M, et al. 2004. On the modeling of sand wave migration. *Journal of Geophysical Research: Oceans*, 109(C4): C04018, doi: [10.1029/2002JC001622](https://doi.org/10.1029/2002JC001622)
- Campmans G H P, Roos P C, De Vriend H J, et al. 2017. Modeling the influence of storms on sand wave formation: A linear stability approach. *Continental Shelf Research*, 137: 103–116, doi: [10.1016/j.csr.2017.02.002](https://doi.org/10.1016/j.csr.2017.02.002)
- Campmans G H P, Roos P C, De Vriend H J, et al. 2018. The influence of storms on sand wave evolution: A nonlinear idealized modeling approach. *Journal of Geophysical Research: Earth Surface*, 123(9): 2070–2086, doi: [10.1029/2018JF004616](https://doi.org/10.1029/2018JF004616)
- Campmans G H P, Roos P C, Van der Sleen N R, et al. 2021. Modeling tidal sand wave recovery after dredging: Effect of different types of dredging strategies. *Coastal Engineering*, 165: 103862, doi: [10.1016/j.coastaleng.2021.103862](https://doi.org/10.1016/j.coastaleng.2021.103862)
- Chen Hsien-Wen, Liu Cho-Teng, Matsuno T, et al. 2016. Temporal variations of volume transport through the Taiwan Strait, as

- identified by three-year measurements. *Continental Shelf Research*, 114: 41–53, doi: [10.1016/j.csr.2015.12.010](https://doi.org/10.1016/j.csr.2015.12.010)
- Chuang Wen-Ssn, Li Hsien-Wen, Tang Tswen Yung, et al. 1993. Observations of the countercurrent on the inshore side of the Kuroshio northeast of Taiwan. *Journal of Oceanography*, 49(5): 581–592, doi: [10.1007/BF02237464](https://doi.org/10.1007/BF02237464)
- Du Xiaoqin, Gao Shu, Li Yan. 2010. Hydrodynamic processes and bedload transport associated with large-scale sandwaves in the Taiwan Strait. *Journal of Coastal Research*, 26(4): 688–698
- Hanes D M. 2012. The genesis of an inter-field marine sandwave and the associated anti-asymmetry migration of neighboring crests. *Geophysical Research Letters*, 39(4): L04402, doi: [10.1029/2011GL050641](https://doi.org/10.1029/2011GL050641)
- Harris P T. 1991. Reversal of subtidal dune asymmetries caused by seasonally reversing wind-driven currents in Torres Strait, northeastern Australia. *Continental Shelf Research*, 11(7): 655–662, doi: [10.1016/0278-4343\(91\)90018-2](https://doi.org/10.1016/0278-4343(91)90018-2)
- Hong Huasheng, Zhang Caiyun, Shang Shangling, et al. 2009. Inter-annual variability of summer coastal upwelling in the Taiwan Strait. *Continental Shelf Research*, 29(2): 479–484, doi: [10.1016/j.csr.2008.11.007](https://doi.org/10.1016/j.csr.2008.11.007)
- Hu Jianyu, Kawamura Hiroshi, Li Chunyan, et al. 2010. Review on current and seawater volume transport through the Taiwan Strait. *Journal of Oceanography*, 66: 591–610, doi: [10.1007/s10872-010-0049-1](https://doi.org/10.1007/s10872-010-0049-1)
- Hu Zifeng, Qi Yiquan, He Xianqiang, et al. 2019. Characterizing surface circulation in the Taiwan Strait during NE monsoon from Geostationary Ocean Color Imager. *Remote Sensing of Environment*, 221: 687–694, doi: [10.1016/j.rse.2018.12.003](https://doi.org/10.1016/j.rse.2018.12.003)
- Hulscher S J M H. 1996. Tidal-induced large-scale regular bed form patterns in a three-dimensional shallow water model. *Journal of Geophysical Research: Oceans*, 101(C9): 20727–20744, doi: [10.1029/96JC01662](https://doi.org/10.1029/96JC01662)
- Hulscher S J M H, Knaapen M A F, Scholl O. 2000. Regeneration of dredged sand waves. *Proceedings of Marine sandwave Dynamics*, 23–24
- IHO. 2008. IHO Standards for Hydrographic Surveys, S-44. 5th ed. Monaco: International Hydrographic Organization, 1–23
- Jan Sen, Chao Shenyu. 2003. Seasonal variation of volume transport in the major inflow region of the Taiwan Strait: the Penghu Channel. *Deep Sea Research Part II: Topical Studies in Oceanography*, 50(6–7): 1117–1126, doi: [10.1016/S0967-0645\(03\)00013-4](https://doi.org/10.1016/S0967-0645(03)00013-4)
- Katoh K, Kume H, Kuroki K, et al. 1998. The development of sand waves and the maintenance of navigation channels in the Bisaneto Sea. In: *Proceedings of the 26th International Conference on Coastal Engineering*. Copenhagen: ASCE, 3490–3502
- Knaapen M A F, Hulscher S J M H. 2002. Regeneration of sand waves after dredging. *Coastal Engineering*, 46(4): 277–289, doi: [10.1016/S0378-3839\(02\)00090-X](https://doi.org/10.1016/S0378-3839(02)00090-X)
- Knaapen M A F, Hulscher S J M H, Scholl O. 2000. Can we predict the growth of sand waves? Hindcast of a field experiment in the Bisaneto Sea, Japan. In: *Proceedings of the 27th International Conference on Coastal Engineering*. Sydney, ASCE, 2661–2671, doi: [10.1061/40549\(276\)208](https://doi.org/10.1061/40549(276)208)
- Li Li, Guo Xiaogang, Liao Enhui, et al. 2018. Subtidal variability in the Taiwan Strait induced by combined forcing of winter monsoon and topography. *Science China Earth Sciences*, 61(4): 483–493, doi: [10.1007/s11430-016-9132-9](https://doi.org/10.1007/s11430-016-9132-9)
- Liu Zhenxia, Xia Dongxing, Berné S, et al. 1998. Tidal deposition systems of China's continental shelf, with special reference to the eastern Bohai Sea. *Marine Geology*, 145(3–4): 225–253, doi: [10.1016/S0025-3227\(97\)00116-3](https://doi.org/10.1016/S0025-3227(97)00116-3)
- McCave I N. 1971. Sand waves in the North Sea off the coast of Holland. *Marine Geology*, 10(3): 199–225, doi: [10.1016/0025-3227\(71\)90063-6](https://doi.org/10.1016/0025-3227(71)90063-6)
- Oey Lie-Yauw, Chang Yu-Lin, Lin Yu Chun, et al. 2014. Cross flows in the Taiwan Strait in winter. *Journal of Physical Oceanography*, 44(3): 801–817, doi: [10.1175/JPO-D-13-0128.s1](https://doi.org/10.1175/JPO-D-13-0128.s1)
- Off T. 1963. Rhythmic linear sand bodies caused by tidal currents. *AAPG Bulletin*, 47(2): 324–341
- Shen Junqiang, Qiu Yun, Guo Xiaogang, et al. 2017. The spatio-temporal variation of wintertime subtidal currents in the western Taiwan Strait. *Acta Oceanologica Sinica*, 36(11): 4–13, doi: [10.1007/s13131-017-1120-1](https://doi.org/10.1007/s13131-017-1120-1)
- Shen Junqiang, Zhang Junpeng, Qiu Yun, et al. 2019. Winter countercurrent in western Taiwan Strait: Characteristics and mechanisms. *Continental Shelf Research*, 172: 1–11, doi: [10.1016/j.csr.2018.11.005](https://doi.org/10.1016/j.csr.2018.11.005)
- Terwindt J H J. 1971. Sand waves in the southern bight of the North Sea. *Marine Geology*, 10(1): 51–67, doi: [10.1016/0025-3227\(71\)90076-4](https://doi.org/10.1016/0025-3227(71)90076-4)
- Van de Meene J W H, Boersma J R, Terwindt J H J. 1996. Sedimentary structures of combined flow deposits from the shoreface-connected ridges along the central Dutch coast. *Marine Geology*, 131(3–4): 151–175, doi: [10.1016/0025-3227\(95\)00074-7](https://doi.org/10.1016/0025-3227(95)00074-7)
- Verboven I. 2017. Regeneration of tidal sand waves after dredging field data analysis, model simulations, and synthesis to dredging strategies [dissertation]. Enschede: University of Twente
- Wang Yuhuai, Jan Sen, Wang Dongping. 2003. Transports and tidal current estimates in the Taiwan Strait from shipboard ADCP observations (1999–2001). *Estuarine, Coastal and Shelf Science*, 57(1–2): 193–199, doi: [10.1016/S0272-7714\(02\)00344-X](https://doi.org/10.1016/S0272-7714(02)00344-X)
- Wang Li, Pawlowicz R, Wu Xiongbin, et al. 2021. Wintertime variability of currents in the southwestern Taiwan Strait. *Journal of Geophysical Research: Oceans*, 126(5): e2020JC016586, doi: [10.1029/2020JC016586](https://doi.org/10.1029/2020JC016586)
- Zhou Jieqiong, Wu Ziyin, Jin Xianglong, et al. 2018. Observations and analysis of giant sand wave fields on the Taiwan Banks, northern South China Sea. *Marine Geology*, 406: 132–141, doi: [10.1016/j.margeo.2018.09.015](https://doi.org/10.1016/j.margeo.2018.09.015)